crystals

MDPI

Communication

Structural and Theoretical Evidence of the Depleted Proton Affinity of the N3-Atom in Acyclovir

Esther Vílchez-Rodríguez [1], Inmaculada Pérez-Toro [1], Antonio Bauzá [2] and Antonio Matilla-Hernández [1,*]

1 Department of Inorganic Chemistry, Faculty of Pharmacy, University of Granada, 18071 Granada, Spain; estervr@correo.ugr.es (E.V.-R.); inptoro@ugr.es (I.P.-T)
2 Department of Chemistry, Faculty of Science, University of the Balearic Islands, Crta. de Valldemossa km 7.5, 07122 Palma de Mallorca (Baleares), Spain; antonio.bauza@uib.es
* Correspondence: amatilla@ugr.es; Tel.: +34-958-243-854

Academic Editors: Thomas Doert and Mathias Wickleder
Received: 27 September 2016; Accepted: 21 October 2016; Published: 29 October 2016

Abstract: The hydronium salt $(H_3O)_2[Cu(N7–acv)_2(H_2O)_2(SO_4)_2]{\cdot}2H_2O$ (1, acv = acyclovir) has been synthesized and characterized by single-crystal X-ray diffraction and spectral methods. Solvated $Cu(OH)_2$ is a by-product of the synthesis. In the all-*trans* centrosymmetric complex anion, (a) the Cu(II) atom exhibits an elongated octahedral coordination; (b) the metal-binding pattern of acyclovir (acv) consists of a Cu–N7(acv) bond plus an (aqua)O–H···O6(acv) interligand interaction; and (c) *trans*-apical/distal sites are occupied by monodentate O–sulfate donor anions. Neutral acyclovir and aqua-proximal ligands occupy the basal positions, stabilizing the metal binding pattern of acv. Each hydronium(1+) ion builds three H-bonds with O-sulfate, O6(acv), and O–alcohol(acv) from three neighboring complex anions. No O atoms of solvent water molecules are involved as acceptors. Theoretical calculations of molecular electrostatic potential surfaces and atomic charges also support that the O-alcohol of the N9(acv) side chain is a better H-acceptor than the N3 or the O-ether atoms of acv.

Keywords: copper(II); mixed-ligand; hydronium; crystal structure; DFT calculations; interligand interactions

1. Introduction

During the past decades, various contributions on metal ion complexes with acyclovir (acv, Figure 1) have been reported. This acyclic guanine nucleoside analog has proved to bind nucleoside phosphorylases [1] as well as several metal ions. Structural knowledge on mixed-ligand metal–acv complexes (see selected reference [2–12]) supports a variety of metal binding patterns (MBPs) and interesting molecular recognition features. So far, the reported MBPs can be summarized as follows: (a) the formation of the M–N7 bond, with [2–9,12] or without [8,10] the cooperation of an intra-molecular interligand A–H···O6(acv) interaction (A=O or N acceptor); (b) the N7,O6-chelation mode [11]; (c) the μ_2-N7,O(ol) (see Figure 1) bridging role [3]; and finally, (d) a multi-functional role featured by the μ_3-N7,O6,O(e)+O(ol), which comprises the bridging, chelating, and tetradentate modes of acv [12].

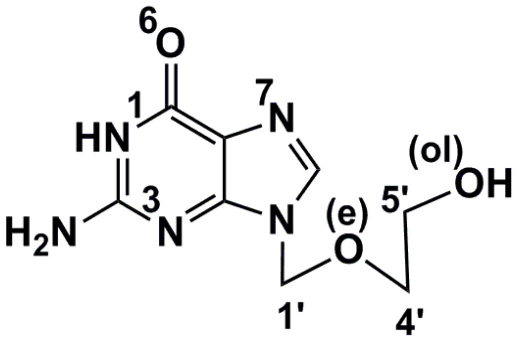

Figure 1. Formula of acyclovir and the numbering used in this work (see also Figure A1).

2. Results and Discussion

As part of our program expanding the frontiers of acv as a ligand, different reactions between acv and metal chelates were performed, using a large variety of tri- and tetra-dentate chelators. An attempt to obtain the ternary complex Cu(II)–DEA–acv (DEA = diethanolamine) yielded a DEA-free greenish powder with a few well-shaped single crystals corresponding to the formula $(H_3O)_2[Cu(acv)_2(H_2O)_2(SO_4)_2]\cdot 2H_2O$ (**1**, 100 K, monoclinic system, space group $P2_1/c$, final R_1 = 0.045. Table A1) along with bluish $Cu(OH)_2$. The *all-trans* centrosymmetric anions (Figures 2 and A2) have symmetry-related pairs of O–aqua, N7–acv, and O–sulfate donor atoms featuring a rather typical elongated-octahedral Cu(II) coordination, type 4 + 2, with bond lengths of Cu–O(aqua) of 1.963(2) Å, of Cu–N7(acv) of 2.018(2) Å, and of Cu–O(sulfate) of 2.427(2) Å, respectively (Table A2). It seems clear that the, shortest strongly-bound Cu–O(aqua) favor the cooperation of each Cu–N7(acv) bond with an intra-molecular interligand (aqua)O1–H1B···O6(acv) interaction (2.615(3) Å, 157.3°) (Table A3), thus leading to the most common MBP of the acv ligand [2–9,12]. This fact imposes the coordination of O–sulfate atoms towards the apical/distal sites of the copper(II) surrounding. In addition, three (hydronium)O–H···O interactions stabilize the structure involving the O6, O(ol), and O(sulfate) atoms from three neighboring complex anions as acceptors, excluding the participation of O-water molecules within the intermolecular network (Table A4, Figures A3 and A4). The novel compound is closely related to the molecular compound all *trans*-$[Cu(acv)_2(H_2O)_2Cl_2]$ [5] where chloride ligands are also moved to the *trans*-apical/distal coordination to favor the cooperation between Cu–N7(acv) bonds and (aqua)O–H···O6(acv) interactions.

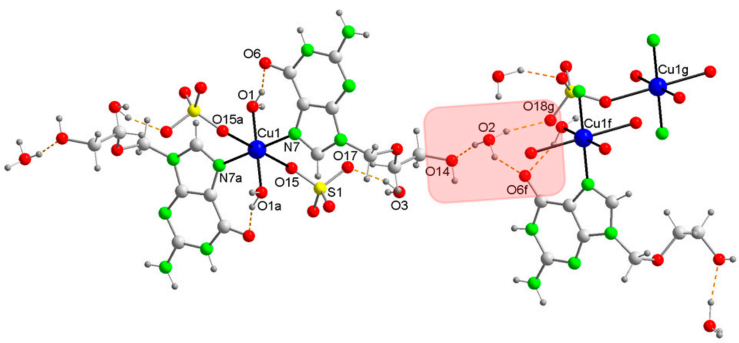

Figure 2. Structure and H-bonding interactions (dashed lines) in **1**. The H_3O^+ ion is H-bonded to O-acceptors of three neighboring complex anions. Symmetry codes: $a = -x, -y + 1, -z; f = x + 1, -y + 1/2, z + 1/2; g = -x + 1, y -1/2, -z + 3/2$.

In the Fourier transform infrared (FT-IR) spectrum of **1** (see also Figure A5 for acv·0.68 H_2O and Figure A6, Table A5), the monodentate sulfate ligands (~C_{3v} symmetry) split the ν_3 mode in two intense bands at 1122 and 1041 cm^{-1}, while only one ν_3 band is observed for the free ion at about

1033–1440 cm^{-1}. Likewise, the sulfate ν_4 mode consists of two medium intensity bands at 652 and 611 cm^{-1}, but only one at 613 cm^{-1} for the free ion [4]. The identification of the hydronium ion by FT-IR spectroscopy is not an easy task. In compound **1**, the H_3O^+ ion seems responsible of the broad absorption (ν_1 and/or ν_3) at ~2743 cm^{-1} and the defined band (ν_4) at 1190 cm^{-1} [13]. The electronic spectra of compound 1 (Figure A8) explain its greenish color (see Appendix A.4).

This structure, therefore, exhibits two uncommon features: (a) the apical/distal copper(II) coordination of the divalent sulfate anions versus the basal coordination of neutral aqua and acv ligands, and (b) the unexpected formation of hydronium(1+) cations instead of the protonation of the N3–acv atom. The molecular electrostatic potential surface (MEPS) was computed in the complex anion (Figure 3, Cartesian coordinates in Table A6) in order to better understand the basis of these features. As expected, the most negative region is located around the sulfate ligands, which are the best candidates to participate in H-bonding interactions with the H_3O^+ ion. Indeed, this is observed in the crystal packing of compound **1**. A comparison of MEPS values at the N3 and O(ol) atoms of the N9-acyclic chain reveals that the most negative electrostatic potential falls at the O(ol) atom, supporting the observed (H_3O^+)O–H···O(ol) interaction, whereas no interaction with (H_3O^+)O–H···N3(acv) is built. To further discuss the ability of the O(ol) atom and the N3(acv) atom, from the acv N9-side chain and the purine-like moiety, respectively, to participate in H-bonding interactions as acceptors, the atomic charges for $[Cu(acv)_2(H_2O)_2(SO_4)_2]^{2-}\cdot 2H_2O$ were also computed. Results computed using two different methods for deriving atomic charges (see ESI for details) yield a more negative charge on the O(ol) atom than on the O(ether) and N3 atoms (Figure 4), in agreement with the experimental results. Therefore, the N3-acv atom is not protonated in the structure due to the significant depletion of its basicity. The steric hindrance on the N3(acv) atom imposed by the acv N9-side chain and ortho-2-amino group should also be considered.

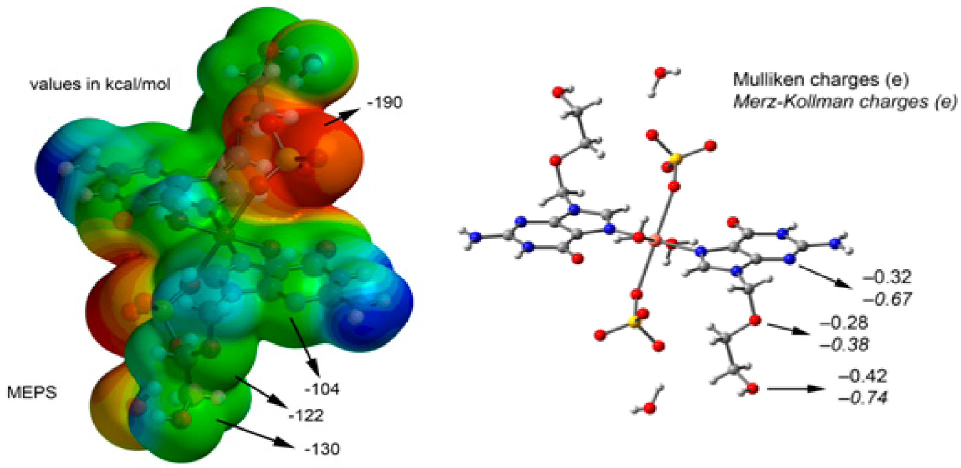

(**a**) (**b**)

Figure 3. Compound **1**: (**a**) molecular electrostatic potential surface (MEPS). The values at selected points of the surface are indicated. Color code: from red to blue, with red being the most negative and blue the most positive values; (**b**) Mulliken and Merz-Kollman charges obtained at the BP86-D3/def2-TZVP level of theory.

We have also evaluated, energetically, the interaction energy of the H_3O^+ ion with the O(ol) atom (observed experimentally) and the hypothetical complex with N3(acv), as indicated in Figure 4 (see Cartesian coordinates in Table A7). The interaction energies in both cases are very large (−88.8 and −88.1 kcal/mol, respectively) due to the strong electrostatic attraction between the counter ions. Interestingly, the complexation energy is slightly more favorable with the O(ol) atom than with N3(acv), in agreement with the experimental observation. We have also evaluated the complexation energy of the solid state assembly commented above in Figure 2 and the theoretical model is depicted in Figure 4c. The interaction energy of this assembly is very large (−100.3 kcal/mol) due to the contribution of both H-bonding interactions and also the pure electrostatic effects.

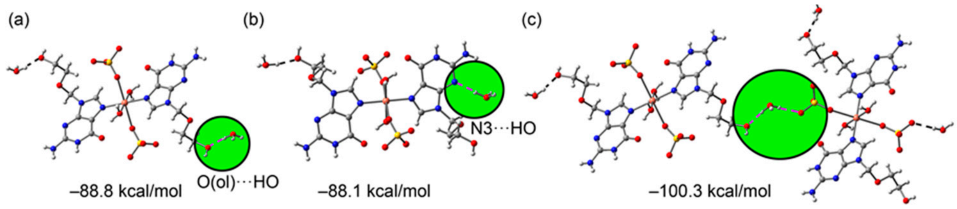

Figure 4. Theoretical models used to evaluate the electrostatic assisted H-bonding interactions in the solid state of compound **1**. (**a**): Interaction of H_3O^+ with O(ol) atom of acv; (**b**): Interaction of H_3O^+ with N3 atom of acv; (**c**): Interaction of H_3O^+ with O(ol) of acv and O-Sulfate atom.

3. Materials and Methods

3.1. Synthesis of Compound 1

Equimolar amounts (0.5 mmol) of $CuSO_4{\cdot}5H_2O$ and DEA were dissolved in 70 mL of methanol. Acyclovir (acv·$0.66H_2O$, 0.5 mmol) was added in small amounts to yield an apple-greenish solution that was filtered into a crystallizing dish. Slow evaporation yields compound **1** and bluish $Cu(OH)_2$. Compound **1** can easily be collected by filtration and dried on a filter paper. Yield: 65%.

3.2. Crystal Structure Determination

A green plate crystal of $(H_3O)_2[Cu(acv)_2(H_2O)_2(SO_4)_2]{\cdot}2H_2O$ was mounted on a glass fiber and used for data collection. Crystal data were collected at 100(2) K, using a Bruker X8 KappaAPEXII diffractometer. Graphite monochromated MoK(α) radiation (λ = 0.71073 Å) was used throughout. The data were processed with APEX2 [14] and corrected for absorption using SADABS (transmissions factors: 1.000—0.907) [15]. The structure was solved by direct methods using the program SHELXS-2013 [16] and refined by full-matrix least-squares techniques against F^2 using SHELXL-2013 [16]. Positional and anisotropic atomic displacement parameters were refined for all non-hydrogen atoms. Hydrogen atoms were located in difference maps and included as fixed contributions riding on attached atoms with isotropic thermal parameters 1.2 times those of their carrier atoms. Criteria of a satisfactory complete analysis were the ratios of the RMS shift to standard deviation less than 0.001 and no significant features in final difference maps. Atomic scattering factors were taken from the International Tables for Crystallography [17]. Molecular graphics were plotted from DIAMOND [18].

3.3. Theoretical Calculations

The energies and atomic charges of the compound included in this study were computed using the BP86-D3 functional [19,20] and def2-TZVP [21] basis set using the crystallographic coordinates within the TURBOMOLE 7.0 program [22]. This level of theory, which includes the latest available dispersion correction (D3) [23], is adequate for studying non-covalent interactions, for which dispersion effects are important. The MEP surfaces were generated using Spartan'10 v. 1.1.0 software [24] using the B3LYP [25–27] method and the 6-31+G* basis set.

Acknowledgments: Support of the Intramural CSIC project 201530E011, the Research Group FQM-283 and the Project MAT2010-15594 of MICINN-Spain are acknowledged. ERDF Funds and Junta de Andalucía support to acquire the FT-IR spectrophotometer Jasco 6300.

Author Contributions: Esther Vílchez-Rodríguez and Inmaculada Pérez-Toro have performed the synthesis of compound and preparation of samples. Antonio Bauzá has performed the MEPS calculations. Data analysis and write manuscript by Antonio Matilla-Hernández. All authors have participated in the discussion of results.

Conflicts of Interest: The authors declare no conflict of interest.

Appendix A

Crystallographic data for **1** has been deposited with the Cambridge Crystallographic Data Centre, CCDC No. 1433120. Copies of this information may be obtained free of charge on application to CCDC, 12 Union Road, Cambridge CB2 1EZ, UK (fax: +44-1223-336-033; email: deposit@ccdc.cam.ac.uk or http://www.ccdc.cam.ac.uk).

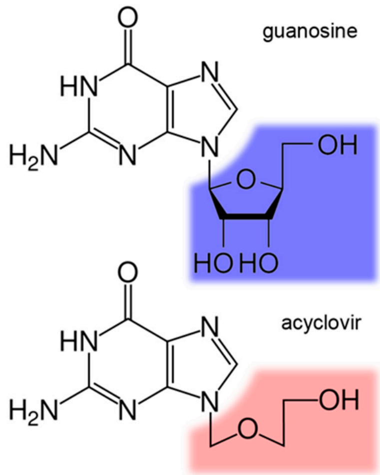

Figure A1. Structural correlation between guanosine and acyclovir.

Appendix A.1. Structural Data

Table A1. Crystal data, structure solution, and refinement of compound **1**.

Identification code	**14jnac876**
Empirical formula	$C_{16}H_{36}CuN_{10}O_{20}S_2$
Formula weight	816.21
Crystal system, space group	Monoclinic, $P2_1/c$
Unit cell dimensions	a = 12.1489(4)Å, α = 90°
	b = 18.2712(5)Å, β = 102.755(1)°
	c = 6.8294(2) Å, γ = 90°
Volume	1478.55(8) $Å^3$
Z, Calculated density	2, 1.833 Mg/m^3
Absorption coefficient	0.987 mm^{-1}
$F(000)$	846
Crystal size	0.100 × 0.080 × 0.040 mm
Theta range for data collection (°)	2.229 to 29.204
Limiting indices	$-15 \leq h \leq 16$, $-24 \leq k \leq 24$, $-9 \leq l \leq 9$
Reflections collected/unique	19,513/3985 [R_{int} = 0.0392]
Completeness to θ = 25.242	99.8%
Absorption correction	Semi-empirical from equivalents
Max. and min. transmission	1.0000 and 0.9069
Refinement method	Full-matrix least-squares on F^2
Data/parameters	3985/223
Goodness-of-fit on F^2	1.092
Final R indices [$I > 2\sigma(I)$]	R_1 = 0.0449, wR_2 = 0.1042
R indices (all data)	R_1 = 0.0559, wR_2 = 0.1099
Largest diff. peak and hole	1.260 and −0.907 e.$Å^{-3}$

Table A2. Coordination bond lengths (Å) and angles (°) for compound **1**.

Bond Lengths (Å) of Compound 1	
Cu(1)–O(1) [a]	1.9630(18)
Cu(1)–O(1)	1.9630(18)
Cu(1)–N(7) [a]	2.018(2)
Cu(1)–N(7)	2.018(2)
Cu(1)–O(15)	2.4271(17)
Cu(1)–O(15) [a]	2.4271(17)
Angles (°) for Compound 1	
O(1) [a]–Cu(1)–O(1)	180.0
O(1) [a]–Cu(1)–N(7) [a]	90.48(8)
O(1)–Cu(1)–N(7) [a]	89.52(8)
O(1) [a]–Cu(1)–N(7)	89.52(8)
O(1)–Cu(1)–N(7)	90.48(8)
N(7) [a]–Cu(1)–N(7)	180.0
O(1) [a]–Cu(1)–O(15)	88.41(7)
O(1)–Cu(1)–O(15)	91.59(7)
N(7) [a]–Cu(1)–O(15)	86.78(7)
N(7)–Cu(1)–O(15)	93.22(7)
O(1) [a]–Cu(1)–O(15) [a]	91.59(7)
O(1)–Cu(1)–O(15) [a]	88.41(7)
N(7) [a]–Cu(1)–O(15) [a]	93.22(7)
N(7)–Cu(1)–O(15) [a]	86.78(7)
O(15)–Cu(1)–O(15) [a]	180.00(8)

Symmetry transformation used to generate equivalent atoms, [a]: $-x$, $-y + 1$, $-z$.

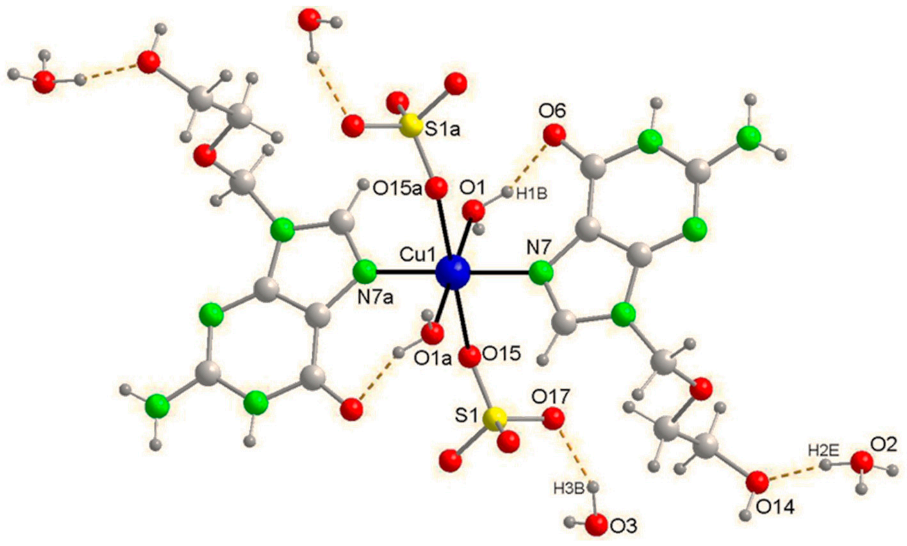

Figure A2. Structure of compound **1**, corresponding to two symmetry-related asymmetric units (symmetry transformation, **a**: $-x$, $-y + 1$, $-z$).

Table A3. Hydrogen bonds for compound **1** (Å, °).

D–H···A	*d*(D–H)	*d*(H···A)	*d*(D···A)	Z(DHA)
O(1)–H(1A)···O(17)	0.87	2.17	2.727(3)	121.3
O(1)–H(1B)···O(6)	0.87	1.79	2.615(3)	157.3
O(14)–H(14)···O(16) [c]	0.84	1.82	2.647(3)	166.2
N(1)–H(1)···O(18) [d]	0.88	1.96	2.832(3)	170.2
N(2)–H(2A)···O(17) [e]	0.88	2.11	2.905(3)	149.4
N(2)–H(2B)···O(15) [d]	0.88	2.08	2.859(3)	147.3
O(2)–H(2C)···O(6) [f]	0.87	2.06	2.825(3)	146.2
O(2)–H(2D)···O(18) [g]	0.87	1.96	2.808(3)	165.5
O(2)–H(2E)···O(14)	0.98	1.82	2.786(3)	170.4
O(3)–H(3A)···O(14) [h]	0.84	2.61	3.124(3)	121.0
O(3)–H(3A)···O(16) [i]	0.84	2.59	3.101(3)	120.2
O(3)–H(3A)···O(2) [j]	0.84	2.48	3.053(4)	125.8
O(3)–H(3B)···O(17)	0.98	1.83	2.751(3)	153.9

Symmetry transformations used to generate equivalent atoms, c: −x + 1, −y + 1, −z + 1; d: −x, y − 1/2, −z + 1/2; e: x, −y + 1/2, z − 1/2; f: x + 1, −y + 1/2, z + 1/2; g: −x + 1, y − 1/2, −z + 3/2; h: −x + 1, −y + 1, −z + 2; i: x, y, z + 1; j: −x + 1,y + 1/2, −z + 3/2.

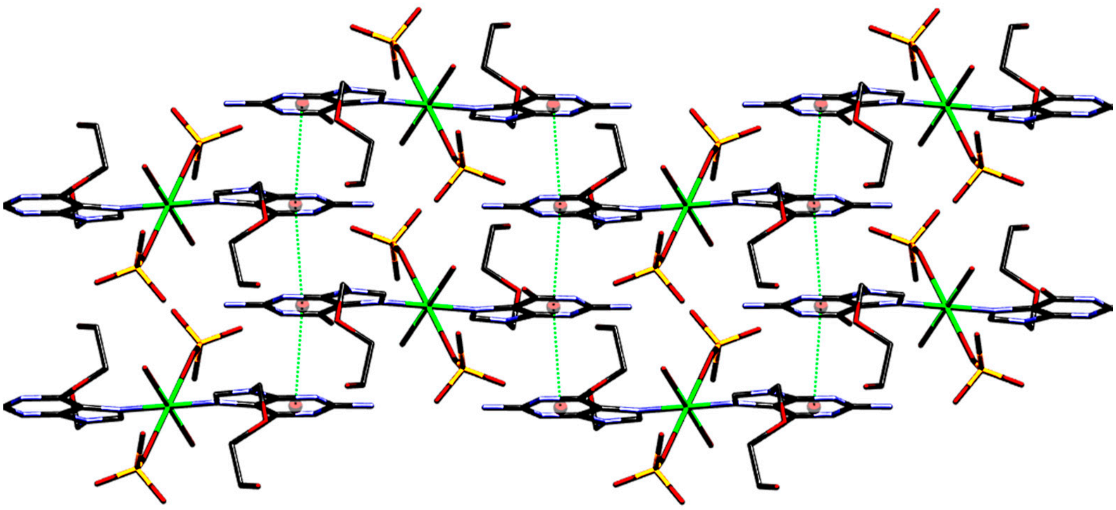

Figure A3. π,π-interactions between the six-membered rings of guanine moieties building 2D frameworks parallel to the bc plane of the crystal.

Table A4. π,π-Staking interaction parameters in the crystal of compound **1** (Å, °).

π···π interactions	Cg(I)···Cg(J)	α
Cg(1)···Cg(1) [e]	3.4235	3.00
Cg(1)···Cg(1) [k]	3.4235	3.00

Cg(1): ring [N(1)/C(2)/N(3)/C(4)/C(5)/C(6)]. Symmetry transformations used to generate equivalent atoms, e: x, −y + 1/2, z − 1/2; k: x, −y + 1/2, z + $\frac{1}{2}$; Cg(I)···Cg(J): distance between ring centroids; α: dihedral angle between planes I and J.

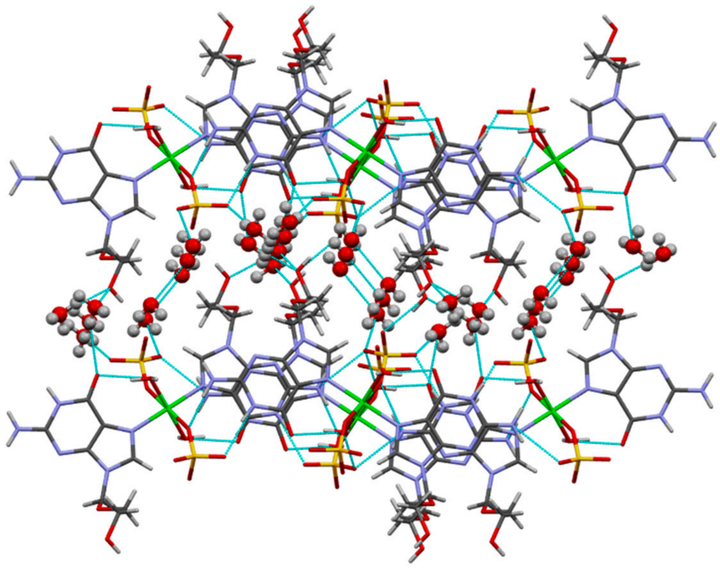

Figure A4. Many H-bonds, some of them involving H_3O+ ions, H_2O molecules, and acv-O(ol)H groups as H-donors, linking the π,π-stacked 2D-layers in a 3D array in the crystal of compound **1**.

Appendix A.2. FT-IR Spectrum

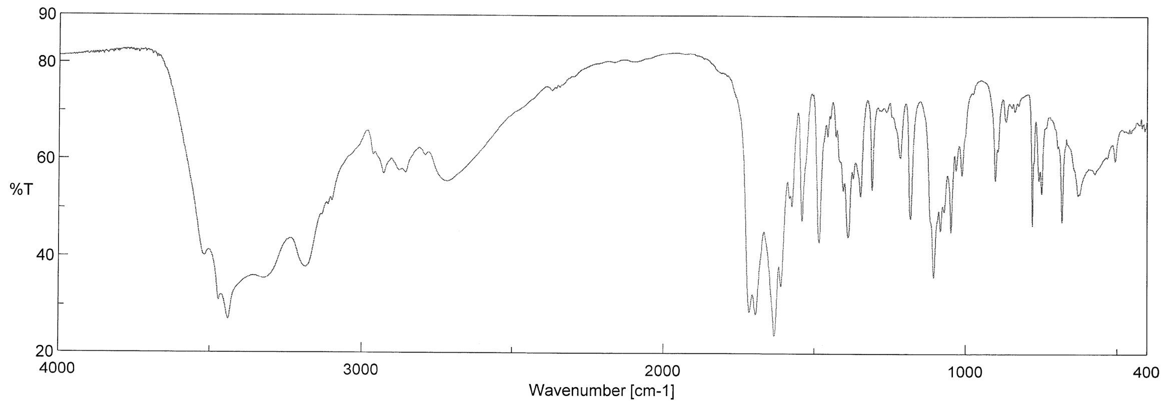

Figure A5. FT-IR spectrum of a commercial sample of acv·0.66 H_2O (KBr disks).

The absorption band of the stretching mode ν(C=O) in various spectra recorded for commercial samples of acv·0.66H_2O splits into two partially-overlapped bands at 1720(3) and 1695(2) cm^{-1}.

In the FT-IR spectra of copper(II) complexes having solvate and/or coordinated acv, this band is located very close to 1695 cm^{-1}. However, this is not the case of compound **1** (see Figure A6), where this ν(C=O) band appears at 1683 cm^{-1} because the exocyclic O6 atom of acv acts twice as an H-acceptor for an intra-molecular and an inter-molecular H-bonding interaction.

An additional band with good diagnostic value is that of the out-of-plane deformation mode δ(O–H) for the terminal alcohol functional group of the N9-side chain, –O(ol)–H, that appears as a more or less defined band near 1387(3) cm^{-1} (see band 33 at 1387 cm^{-1}).

However, attention must be paid if the studied copper(II) complexes contain nitrate or carboxylate anions, which produce stretching bands near to 1385 cm^{-1}.

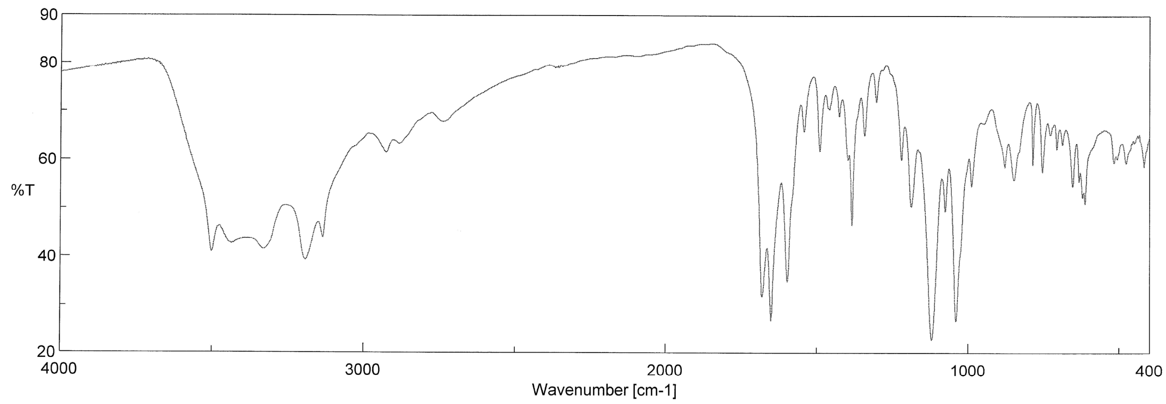

Figure A6. FT-IR spectrum of compound **1**.

Table A5. Assignation peaks of compound **1**.

Ligand or Solvent	Chromophore	Mode	Wavenumber (cm^{-1})	Band Number in the Read Spectrum
H_3O^+ ion	H_3O^+	$\nu_1(A_1)$ and $\nu_3(E)$	2743 (broad)	9
		$\nu_2(A_1)$	1190	24
H_2O	H_2O	ν_{as}	3430	2
		ν_s	~3450	N/M *
		δ	1652	11
acv	O(ol)–H	ν	3502	1
		δ	1385	20
	–N(2)H_2	ν_{as}	3327	3
		ν_s	3195	4
		δ	1598	12
	–N(1)–H	ν	3139	5
		δ	1541	14
	–C=O(6)	ν	1683	10 **
	C–O(e)–C	ν_{as}	1178	26
sulfate	SO_4^{2-}	ν_3	1122	25
			1041	27
		ν_1	989	28
		ν_4	652	36
			611	39
		ν_2	448	44

* N/M = not measured. ** This band usually splits in two at 1720(3) and 1695(3) cm^{-1} in the spectra of acv·0.66H_2O samples, and appear at about 1695 cm^{-1} in the spectra of Cu(II)-acv complexes with monodentate acv ligands. Note that, in compound **1**, the O6 atom of acv is involved as an acceptor in two H-bonds.

Appendix A.3. ESR Spectrum and Magnetic Properties of Compound ***1***

X-band ESR (Electronic Spin Resonance) measurements were carried out on a Bruker ELEXSYS 500 spectrometer equipped with a super-high-Q resonator ER-4123-SHQ. For Q-band studies, ESR spectra were recorded on a Bruker EMX system equipped with an ER-510-QT resonator. The room temperature X-band powder spectra are not well resolved due to a rather large line width. However at the Q-band (Figure A7) the signal is clearly characteristic of an axial g tensor with the following main values: $g_{||}$ = 2.339, and $g_{\perp}$ =2.086 (computer simulation: WINEPR-Simfonia, version 1.5, Bruker Analytische Messtechnik GmbH.

The g values are typical of Cu(II) ions in distorted octahedral environments in good agreement with the structural characteristics of the CuN_2O_4 chromophore. Moreover, the lowest g deviates appreciably from the free electron value (g_0 = 2.0023) indicating a dx2-y2 ground state, as corresponds to an axially-elongated octahedral environment for Cu(II) ions. The absence of well-resolved hyperfine lines contrasts with the structurally monomeric nature of the compound. The collapse of the hyperfine structure usually indicates the presence of long-range exchange coupling. The hydrogen bonding and/or the π,π-stacking of the acyclovir rings can provide the necessary exchange pathway.

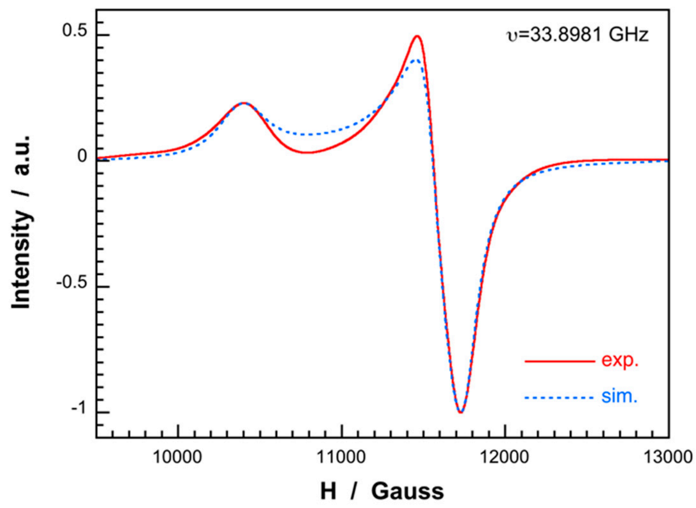

Figure A7. Q-band ESR powder spectrum of compound **1** registered at room temperature. Dotted line is the best fit; see text for the fitting parameters.

Variable temperature (5–300 K) magnetic susceptibility measurements on polycrystalline samples were carried out with a Quantum Design MPMS-7 SQUID magnetometer under a magnetic field of 0.1 T. The experimental susceptibilities were corrected for the diamagnetism of the constituent atoms by using Pascal's tables. Magnetic susceptibility data show typical Curie–Weiss behavior. The calculated Curie constant (Cm = 0.44 $cm^3 \cdot K/mol$) is in good agreement with the *g*-values obtained from ESR experiments (g = 2.170; Cm = 0.442). The Weiss temperature intercept is close to zero indicating that magnetic interactions between Cu(II) centers are very weak.

Appendix A.4. Electronic Spectrum of Compound ***1***

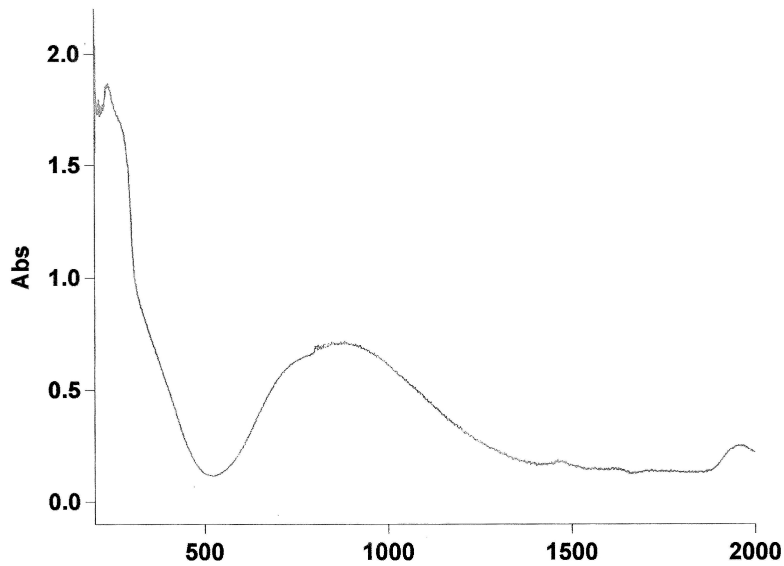

Figure A8. Electronic spectrum (diffuse reflectance) of compound **1** (Abs. vs: wavelength, nm.).

The asymmetric *d-d* band spectrum exhibits a maximum of absorption at 881 nm (11,350 cm^{-1}) with an intensity barycenter at 950 nm (10,525 cm^{-1}) according to the apple-greenish color of compound **1**.

For comparison, the electronic spectrum for a blue solution of the aqua-complex ion, $[Cu(H_2O)_6]^{2+}$, shows a ν_{max} near 800 nm (~12,500 cm^{-1}).

Appendix A.5. Cartesian Coordinates

Table A6. Model in Figure 3

Cu	0.00000055	9.13598209	−0.00000659
S	1.95000055	10.31898209	2.88599341
O	−1.55199945	8.26798209	0.83299341
H	−1.60699945	8.50198209	1.67299341
H	−1.46399945	7.39998209	0.78199341
O	−1.59299945	5.76898209	0.06499341
O	4.64200055	5.81798209	2.09099341
O	5.76400055	6.14698209	4.77399341
H	6.38900055	6.69498209	4.64399341
O	0.71900055	10.04798209	2.13099341
O	3.14500055	10.12898209	2.04599341
O	2.01700055	9.38598209	4.04799341
O	1.90700000	11.71500000	3.40000000
N	−0.21299945	3.97698209	0.19599341
H	−0.92299945	3.45898209	0.14899341
N	1.00800055	2.02198209	0.31099341
H	1.76200055	1.57498209	0.37999341
H	0.24400055	1.58798209	0.24399341
N	2.16200055	4.02698209	0.40799341
N	1.08500055	7.44998209	0.22599341
N	2.97700055	6.29598209	0.45999341
C	1.02000055	3.35598209	0.30799341
C	1.97600055	5.35998209	0.36699341
C	0.79600055	6.08098209	0.22499341
C	−0.42199945	5.34098209	0.15099341
C	2.38500055	7.52198209	0.37599341
H	2.86300055	8.34098209	0.42199341
C	4.39300055	6.03698209	0.72299341
H	4.68000055	5.24198209	0.20799341
H	4.92900055	6.80998209	0.41299341
C	4.54000055	7.03898209	2.85799341
H	3.70400055	7.51498209	2.61799341
−H	5.30400055	7.63198209	2.64799341
C	4.53600055	6.71398209	4.32899341
H	4.35800055	7.54198209	4.84099341
H	3.80100055	6.07898209	4.51699341
S	−1.94999945	7.95198209	−2.88600659
O	1.55200055	10.00298209	−0.83300659
H	1.60700055	9.76998209	−1.67300659
H	1.46400055	10.87098209	−0.78200659
O	1.59300055	12.50198209	−0.06500659
O	−4.64199945	12.45298209	−2.09100659
O	−5.76399945	12.12398209	−4.77400659
H	−6.38899945	11.57698209	−4.64400659
O	−0.71899945	8.22298209	−2.13100659
O	−3.14499945	8.14198209	−2.04600659
O	−2.01699945	8.88498209	−4.04800659
O	−1.90699945	6.55698209	−3.40000659

Table A6. *Cont.*

N	0.21300055	14.29398209	−0.19600659
H	0.92300055	14.81198209	−0.14900659
N	−1.00799945	16.24898209	−0.31100659
H	−1.76199945	16.69598209	−0.38000659
H	−0.24399945	16.68298209	−0.24400659
N	−2.16199945	14.24398209	−0.40800659
N	−1.08499945	10.82198209	−0.22600659
N	−2.97699945	11.97498209	−0.46000659
C	−1.01999945	14.91498209	−0.30800659
C	−1.97599945	12.91198209	−0.36700659
C	−0.79599945	12.18998209	−0.22500659
C	0.42200055	12.92998209	−0.15100659
C	−2.38499945	10.74898209	−0.37600659
H	−2.86299945	9.92998209	−0.42200659
C	−4.39299945	12.23398209	−0.72300659
H	−4.67999945	13.02898209	−0.20800659
H	−4.92899945	11.46198209	−0.41300659
C	−4.53999945	11.23198209	−2.85800659
H	−3.70399945	10.75598209	−2.61800659
H	−5.30399945	10.63898209	−2.64800659
C	−4.53599945	11.55698209	−4.32900659
H	−4.35799945	10.72898209	−4.84100659
H	−3.80099945	12.19198209	−4.51700659
O	3.53500000	10.00600000	6.25700000
H	2.95000000	10.55300000	6.51100000
H	3.16700000	9.55200000	5.46800000
O	−3.53500000	8.26500000	−6.25700000
H	−2.95000000	7.71800000	−6.51100000
H	−3.16700000	8.71900000	−5.46800000

Table A7. Models in Figure 4

	(a)		
Cu	0.000	9.136	0.000
S	1.950	10.319	2.886
O	−1.552	8.268	0.833
H	−1.607	8.502	1.673
H	−1.464	7.400	0.782
O	−1.593	5.769	0.065
O	4.642	5.818	2.091
O	5.764	6.147	4.774
H	6.389	6.695	4.644
O	0.719	10.048	2.131
O	3.145	10.129	2.046
O	2.017	9.386	4.048
O	1.907	11.715	3.400
N	−0.213	3.977	0.196
H	−0.923	3.459	0.149
N	1.008	2.022	0.311
H	1.762	1.575	0.380
H	0.244	1.588	0.244
N	2.162	4.027	0.408
N	1.085	7.450	0.226
N	2.977	6.296	0.460
C	1.020	3.356	0.308
C	1.976	5.360	0.367
C	0.796	6.081	0.225
C	−0.422	5.341	0.151

Table A7. *Cont.*

C	2.385	7.522	0.376
H	2.863	8.341	0.422
C	4.393	6.037	0.723
H	4.680	5.242	0.208
H	4.929	6.810	0.413
C	4.540	7.039	2.858
H	3.704	7.515	2.618
H	5.304	7.632	2.648
C	4.536	6.714	4.329
H	4.358	7.542	4.841
H	3.801	6.079	4.517
S	−1.950	7.952	−2.886
O	1.552	10.003	−0.833
H	1.607	9.770	−1.673
H	1.464	10.871	−0.782
O	1.593	12.502	−0.065
O	−4.642	12.453	−2.091
O	−5.764	12.124	−4.774
H	−6.389	11.577	−4.644
O	−0.719	8.223	−2.131
O	−3.145	8.142	−2.046
O	−2.017	8.885	−4.048
O	−1.906	6.556	−3.400
N	0.213	14.294	−0.196
H	0.923	14.812	−0.149
N	−1.008	16.249	−0.311
H	−1.762	16.696	−0.380
H	−0.244	16.683	−0.244
N	−2.162	14.244	−0.408
N	−1.085	10.822	−0.226
N	−2.977	11.975	−0.460
C	−1.020	14.915	−0.308
C	−1.976	12.912	−0.367
C	−0.796	12.190	−0.225
C	0.422	12.930	−0.151
C	−2.385	10.749	−0.376
H	−2.863	9.930	−0.422
C	−4.393	12.234	−0.723
H	−4.680	13.029	−0.208
H	−4.929	11.462	−0.413
C	−4.540	11.232	−2.858
H	−3.704	10.756	−2.618
H	−5.304	10.639	−2.648
C	−4.536	11.557	−4.329
H	−4.358	10.729	−4.841
H	−3.801	12.192	−4.517
H	7.901	4.003	3.867
H	7.245	3.409	4.980
H	6.560	4.557	4.397
O	−7.129	14.485	−4.204
H	−7.901	14.268	−3.867
H	−7.245	14.862	−4.980
H	−6.560	13.714	−4.397
	(b)		
Cu	0.00000000	9.13600000	0.00000000
S	1.95000000	10.31900000	2.88600000
O	−1.55200000	8.26800000	0.83300000
H	−1.60700000	8.50200000	1.67300000
H	−1.46400000	7.40000000	0.78200000
O	−1.59300000	5.76900000	0.06500000
O	4.64200000	5.81800000	2.09100000

Table A7. *Cont.*

O	5.76400000	6.14700000	4.77400000
H	6.38900000	6.69500000	4.64400000
O	0.71900000	10.04800000	2.13100000
O	3.14500000	10.12900000	2.04600000
O	2.01700000	9.38600000	4.04800000
O	1.90699945	11.71501791	3.40000659
N	−0.21300000	3.97700000	0.19600000
H	−0.92300000	3.45900000	0.14900000
N	1.00800000	2.02200000	0.31100000
H	1.76200000	1.57500000	0.38000000
H	0.24400000	1.58800000	0.24400000
N	2.16200000	4.02700000	0.40800000
N	1.08500000	7.45000000	0.22600000
N	2.97700000	6.29600000	0.46000000
C	1.02000000	3.35600000	0.30800000
C	1.97600000	5.36000000	0.36700000
C	0.79600000	6.08100000	0.22500000
C	−0.42200000	5.34100000	0.15100000
C	2.38500000	7.52200000	0.37600000
H	2.86300000	8.34100000	0.42200000
C	4.39300000	6.03700000	0.72300000
H	4.68000000	5.24200000	0.20800000
H	4.92900000	6.81000000	0.41300000
C	4.54000000	7.03900000	2.85800000
H	3.70400000	7.51500000	2.61800000
H	5.30400000	7.63200000	2.64800000
C	4.53600000	6.71400000	4.32900000
H	4.35800000	7.54200000	4.84100000
H	3.80100000	6.07900000	4.51700000
S	−1.95000000	7.95200000	−2.88600000
O	1.55200000	10.00300000	−0.83300000
H	1.60700000	9.77000000	−1.67300000
H	1.46400000	10.87100000	−0.78200000
O	1.59300000	12.50200000	−0.06500000
O	−4.64200000	12.45300000	−2.09100000
O	−5.76400000	12.12400000	−4.77400000
H	−6.38900000	11.57700000	−4.64400000
O	−0.71900000	8.22300000	−2.13100000
O	−3.14500000	8.14200000	−2.04600000
O	−2.01700000	8.88500000	−4.04800000
O	−1.90700000	6.55700000	−3.40000000
N	0.21300000	14.29400000	−0.19600000
H	0.92300000	14.81200000	−0.14900000
N	−1.00800000	16.24900000	−0.31100000
H	−1.76200000	16.69600000	−0.38000000
H	−0.24400000	16.68300000	−0.24400000
N	−2.16200000	14.24400000	−0.40800000
N	−1.08500000	10.82200000	−0.22600000
N	−2.97700000	11.97500000	−0.46000000
C	−1.02000000	14.91500000	−0.30800000
C	−1.97600000	12.91200000	−0.36700000
C	−0.79600000	12.19000000	−0.22500000
C	0.42200000	12.93000000	−0.15100000
C	−2.38500000	10.74900000	−0.37600000
H	−2.86300000	9.93000000	−0.42200000
C	−4.39300000	12.23400000	−0.72300000
H	−4.68000000	13.02900000	−0.20800000
H	−4.92900000	11.46200000	−0.41300000
C	−4.54000000	11.23200000	−2.85800000
H	−3.70400000	10.75600000	−2.61800000

Table A7. *Cont.*

H	−5.30400000	10.63900000	−2.64800000
C	−4.53600000	11.55700000	−4.32900000
H	−4.35800000	10.72900000	−4.84100000
H	−3.80100000	12.19200000	−4.51700000
O	7.12900000	3.78600000	4.20400000
H	7.90100000	4.00300000	3.86700000
H	7.24500000	3.40900000	4.98000000
H	6.56000000	4.55700000	4.39700000
O	−4.65114130	15.47000153	−0.72450806
H	−4.64493571	15.98253054	−1.42730071
H	−4.75966993	15.95560247	−0.01024322
H	−3.80193352	15.01038869	−0.57267532
		(c)	
Cu	0.000	9.136	0.000
S	1.950	10.319	2.886
O	−1.552	8.268	0.833
H	−1.607	8.502	1.673
H	−1.464	7.400	0.782
O	−1.593	5.769	0.065
O	4.642	5.818	2.091
O	5.764	6.147	4.774
H	6.389	6.695	4.644
O	0.719	10.048	2.131
O	3.145	10.129	2.046
O	2.017	9.386	4.048
O	1.907	11.715	3.400
N	−0.213	3.977	0.196
H	−0.923	3.459	0.149
N	1.008	2.022	0.311
H	1.762	1.575	0.380
H	0.244	1.588	0.244
N	2.162	4.027	0.408
N	1.085	7.450	0.226
N	2.977	6.296	0.460
C	1.020	3.356	0.308
C	1.976	5.360	0.367
C	0.796	6.081	0.225
C	−0.422	5.341	0.151
C	2.385	7.522	0.376
H	2.863	8.341	0.422
C	4.393	6.037	0.723
H	4.680	5.242	0.208
H	4.929	6.810	0.413
C	4.540	7.039	2.858
H	3.704	7.515	2.618
H	5.304	7.632	2.648
C	4.536	6.714	4.329
H	4.358	7.542	4.841
H	3.801	6.079	4.517
S	−1.950	7.952	−2.886
O	1.552	10.003	−0.833
H	1.607	9.770	−1.673
H	1.464	10.871	−0.782
O	1.593	12.502	−0.065
O	−4.642	12.453	−2.091
O	−5.764	12.124	−4.774
H	−6.389	11.577	−4.644
O	−0.719	8.223	−2.131
O	−3.145	8.142	−2.046

Table A7. *Cont.*

O	−2.017	8.885	−4.048
O	−1.906	6.556	−3.400
N	0.213	14.294	−0.196
H	0.923	14.812	−0.149
N	−1.008	16.249	−0.311
H	−1.762	16.696	−0.380
H	−0.244	16.683	−0.244
N	−2.162	14.244	−0.408
N	−1.085	10.822	−0.226
N	−2.977	11.975	−0.460
C	−1.020	14.915	−0.308
C	−1.976	12.912	−0.367
C	−0.796	12.190	−0.225
C	0.422	12.930	−0.151
C	−2.385	10.749	−0.376
H	−2.863	9.930	−0.422
C	−4.393	12.234	−0.723
H	−4.680	13.029	−0.208
H	−4.929	11.462	−0.413
C	−4.540	11.232	−2.858
H	−3.704	10.756	−2.618
H	−5.304	10.639	−2.648
C	−4.536	11.557	−4.329
H	−4.358	10.729	−4.841
H	−3.801	12.192	−4.517
O	7.129	3.786	4.204
H	7.901	4.003	3.867
H	7.245	3.409	4.980
H	6.560	4.557	4.397
O	−7.129	14.485	−4.204
H	−7.901	14.268	−3.867
H	−7.245	14.862	−4.980
H	−6.560	13.714	−4.397
C	9.887	0.000	9.991
S	7.937	1.183	7.106
O	11.439	−0.867	9.159
H	11.494	−0.634	8.318
H	11.351	−1.736	9.209
O	11.480	−3.366	9.927
O	5.245	−3.317	7.900
O	4.123	−2.988	5.217
H	3.498	−2.441	5.347
O	9.168	0.912	7.860
O	6.742	0.993	7.946
O	7.870	0.250	5.943
O	7.980	2.579	6.592
N	10.100	−5.158	9.795
H	10.810	−5.677	9.842
N	8.880	−7.114	9.680
H	8.125	−7.561	9.612
H	9.644	−7.548	9.747
N	7.725	−5.108	9.583
N	8.802	−1.686	9.765
N	6.910	−2.839	9.532
C	8.867	−5.780	9.683
C	7.911	−3.776	9.624
C	9.091	−3.054	9.766
C	10.309	−3.795	9.841
C	7.503	−1.613	9.615

Table A7. *Cont.*

H	7.024	−0.795	9.570
C	5.494	−3.099	9.269
H	5.207	−3.894	9.783
H	4.958	−2.326	9.578
C	5.348	−2.097	7.134
H	6.183	−1.621	7.374
H	4.583	−1.504	7.344
C	5.352	−2.421	5.662
H	5.529	−1.593	5.150
H	6.087	−3.057	5.475
S	11.837	−1.183	12.877
O	8.335	0.867	10.824
H	8.280	0.634	11.665
H	8.424	1.736	10.773
O	8.295	3.366	10.056
O	14.529	3.317	12.082
O	15.651	2.988	14.765
H	16.276	2.441	14.635
O	10.606	−0.912	12.122
O	13.032	−0.993	12.037
O	11.904	−0.250	14.040
O	11.794	−2.579	13.391
N	9.674	5.158	10.187
H	8.964	5.677	10.141
N	10.895	7.114	10.302
H	11.649	7.561	10.371
H	10.131	7.548	10.236
N	12.049	5.108	10.400
N	10.972	1.686	10.218
N	12.865	2.839	10.451
C	10.907	5.780	10.300
C	11.863	3.776	10.358
C	10.683	3.054	10.216
C	9.466	3.795	10.142
C	12.272	1.613	10.368
H	12.750	0.795	10.413
C	14.281	3.099	10.714
H	14.567	3.894	10.200
H	14.816	2.326	10.404
C	14.427	2.097	12.849
H	13.592	1.621	12.609
H	15.191	1.504	12.639
C	14.423	2.421	14.320
H	14.245	1.593	14.832
H	13.688	3.057	14.508
O	12.646	−3.786	15.779
H	11.873	−4.003	16.115
H	12.530	−3.409	15.003
H	13.214	−4.557	15.586
O	2.759	−5.350	5.788
H	1.986	−5.132	6.124
H	2.643	−5.726	5.012
H	3.327	−4.579	5.594

References

1. Caceres, R.A.; Timmers, L.F.S.M.; Ducati, R.G.; da Silva, D.O.N.; Basso, L.A.; de Azevedo, W.F., Jr.; Santos, D.S. Crystal structure and molecular dynamics studies of purine nucleoside phosphorylase from Mycobacterium tuberculosis associated with acyclovir. *Biochimie* **2011**, *94*, 155–165. [CrossRef] [PubMed]

2. Grabner, S.; Plavec, J.; Bukovec, N.; Di Leo, D.; Cini, R.; Natile, G. Synthesis and structural characterization of platinum(II)-acyclovir complexes. *J. Chem. Soc. Dalton Trans.* **1998**, 1447–1452. [CrossRef]
3. Garcia-Raso, A.; Fiol, J.J.; Badenas, F.; Cons, R.; Terron, A.; Quiros, M. Synthesis and structural characteristics of metal–acyclovir (ACV) complexes: [Ni(or Co)$(ACV)_2(H_2O)_4]Cl_2 \cdot 2ACV$, $[Zn(ACV)Cl_2(H_2O)]$, $[Cd(ACV)Cl_2] \cdot H_2O$ and $[\{Hg(ACV)Cl_2\}_x]$. Recognition of acyclovir by Ni–ACV. *J. Chem. Soc. Dalton Trans.* **1999**, 167–174. [CrossRef]
4. Barceló-Oliver, M.; Terrón, A.; García-Raso, A.; Fiol, J.J.; Molins, E.; Miravitlles, C. Ternary complexes metal [Co(II), Ni(II), Cu(II) and Zn(II)]–ortho-iodohippurate (I-hip)–acyclovir. X-ray characterization of isostructural $[(Co, Ni\ or\ Zn)(I-hip)_2(ACV)(H_2O)_3]$ with stacking as a recognition factor. *J. Inorg. Biochem.* **2004**, *98*, 1703–1711. [CrossRef] [PubMed]
5. Blažič, B.; Turel, I.; Bukovec, N.; Bukovec, P.; Lazarini, F. Synthesis and structure of diaquadichlorobis {9−[(2−hydroxyethoxy)methyl]guanine} copper(II). *J. Inorg. Biochem.* **1993**, *51*, 737–744. [CrossRef]
6. Turel, I.; Pečanac, M.; Golobič, A.; Alessio, E.; Serli, B. Novel RuIII-DMSO Complexes of the Antiherpes Drug Acyclovir. *Eur. J. Inorg. Chem.* **2002**, 1928–1931. [CrossRef]
7. Turel, I.; Pečanac, M.; Golobič, A.; Alessio, E.; Serli, B.; Bergamo, A.; Sava, G. Solution, solid state and biological characterization of ruthenium(III)-DMSO complexes with purine base derivatives. *J. Inorg. Biochem.* **2004**, *98*, 393–401. [CrossRef] [PubMed]
8. Brandi-Blanco, M.P.; Choquesillo-Lazarte, D.; Domínguez-Martín, A.; González-Pérez, J.M.; Castiñeiras, A.; Niclós-Gutiérrez, J. Metal ion binding patterns of acyclovir: Molecular recognition between this antiviral agent and copper(II) chelates with iminodiacetate or glycylglycinate. *J. Inorg. Biochem.* **2011**, *105*, 616–623. [CrossRef] [PubMed]
9. Pérez-Toro, I.; Domínguez-Martín, A.; Choquesillo-Lazarte, D.; Vílchez-Rodríguez, E.; González-Pérez, J.M.; Castiñeiras, A.; Niclós-Gutiérrez, J. Lights and shadows in the challenge of binding acyclovir, a synthetic purine-like nucleoside with antiviral activity, at an apical–distal coordination site in copper(II)-polyamine chelates. *J. Inorg. Biochem.* **2015**, *148*, 84–92. [CrossRef] [PubMed]
10. Sinur, A.; Grabner, S. A Platinum(II) Diammine Complex: *Cis*-$[Pt(C_8H_{11}N_5O_3)_2(NH_3)_2]Cl_2 \cdot 2H_2O$. *Acta Crystallogr.* **1995**, *C51*, 1769–1772. [CrossRef]
11. Turel, I.; Anderson, B.; Sletten, E.; White, A.J.P.; Williams, D.J. New studies in the copper(II) acyclovir (acv) system. NMR relaxation studies and the X-ray crystal structure of $[Cu(acv)_2(H_2O)_2](NO_3)_2$. *Polyhedron* **1998**, *17*, 4195–4201. [CrossRef]
12. Vílchez-Rodríguez, E.; Choquesillo-Lazarte, D.; Domínguez-Martín, A.; Pérez-Toro, I.; Matilla-Hernández, A.; González-Pérez, J.M.; Castiñeiras, A.; Niclós-Gutiérrez, J. Synthetic purine-nucleoside analogs as useful ligands: Looking at the coordination chemistry and metal binding patterns of acyclovir. *J. Coord. Chem. Rev.* **2016**, in Press.
13. Nakamoto, K. *Infrared and Raman Spectra of Inorganic and Coordination Compounds*, Part A, 6th ed.; Wiley: New York, NY, USA, 2009; pp. 173–176.
14. *APEX2 Software, v2010.3–0*; Bruker AXS Inc.: Madison, WI, USA, 2010.
15. Sheldrick, G.M. *SADABS—Program for Empirical Absorption Correction of Area Detector Data*; University of Goettingen: Göttingen, Germany, 1997.
16. Sheldrick, G.M. A short history of SHELX. *Acta Crystallogr.* **2008**, *A64*, 112–122. [CrossRef] [PubMed]
17. Wilson, A.J.C. *International Tables for Crystallography, Vol. C*; Kluwer Academic Publishers: Dordrecht, Netherlands, 1995.
18. Putz, H.; Brandenburg, K. DIAMOND—Crystal and Molecular Structure Visualization. Crystal Impact GbR: Bonn, Germany. Available online: http://www.crystalimpact.com/diamond (accessed on 22 October 2016).
19. Becke, A.D. Density-functional exchange-energy approximation with correct asymptotic behavior. *Phys. Rev. A* **1988**, *38*, 3098–3100. [CrossRef]
20. Perdew, J.P. Density-functional approximation for the correlation energy of the inhomogeneous electron gas. *Phys. Rev. B* **1986**, *33*, 8822–8824. [CrossRef]
21. Weigend, F.; Ahlrichs, R. Balanced basis sets of split valence, triple zeta valence and quadruple zeta valence quality for H to Rn: Design and assessment of accuracy. *Phys. Chem. Chem. Phys.* **2005**, *7*, 3297–3305. [CrossRef] [PubMed]
22. Ahlrichs, R.; Bär, M.; Häser, M.; Horn, H.; Kölmel, C. Electronic structure calculations on workstation computers: The program system turbomole. *Chem. Phys. Lett.* **1989**, *162*, 165–169. [CrossRef]

23. Grimme, S.; Antony, J.; Ehrlich, S.; Krieg, H. A consistent and accurate ab initio parameterization of density functional dispersion correction (DFT-D) for the 94 elements H-Pu. *J. Chem. Phys.* **2010**, *132*, 154104. [CrossRef] [PubMed]
24. *Spartan'10, v. 1.1.0*; Wavefunction Inc.: Irvin, CA, USA, 2013.
25. Becke, A.D. Density-functional thermochemistry. III. The role of exact exchange. *J. Chem. Phys.* **1993**, *98*, 5648–5652. [CrossRef]
26. Lee, C.; Yang, W.; Parr, R.G. Development of the Colle-Salvetti correlation-energy formula into a functional of the electron density. *Phys. Rev. B* **1988**, *37*, 785–789. [CrossRef]
27. Rassolov, V.A.; Pople, J.A.; Ratner, M.A.; Windus, T.L. 6–31G* basis set for atoms K through Zn. *J. Chem. Phys.* **1998**, *109*, 1223–1229. [CrossRef]